Two-Dimensional Localization of Exciton Polaritons in Microcavities

O. A. Egorov,[1,2] A. V. Gorbach,[1] F. Lederer,[2] and D. V. Skryabin[1]

[1]*Centre for Photonics and Photonic Materials, Department of Physics, University of Bath, Bath BA2 7AY, United Kingdom*

[2]*Institute of Condensed Matter Theory and Solid State Optics, Friedrich-Schiller-Universität Jena, Max-Wien-Platz 1, 07743 Jena, Germany*

(Received 3 March 2010; published 12 August 2010)

We report two-dimensional localization of exciton polaritons in a coherently pumped planar semiconductor microcavity operating in the strong-coupling regime. Two-dimensional polariton solitons exist despite the opposite dispersion signs along the orthogonal in plane directions. Nonlinearities compensating the opposing dispersions have different physical origins and are due to the repulsion of polaritons on one side and due to parametric four-wave mixing on the other. Both of these nonlinearities can support their respective families of one-dimensional solitons, which coexist with each other and with the two-dimensional solitons.

DOI: 10.1103/PhysRevLett.105.073903 PACS numbers: 42.65.Tg, 05.45.Yv, 42.65.Sf, 71.36.+c

The research into the physical principles of the existence and evolution of localized structures (LSs) or solitons in nonlinear systems spans many branches of physical sciences including optics, fluid dynamics, particle physics, and biology [1]. Depending on the physical setting, localization can occur in one, two, or three dimensions. Changing the dimension is often accompanied by qualitative changes of the LS properties of localized structures and opens up new research avenues [2].

One of the qualitative principles underpinning the LS formation is that the dispersion induced broadening is compensated by a nonlinearity of the appropriate sign, and if loss is present, then it has to be compensated by an external energy source. Most generally, if dispersive spreading happens as for quantum mechanical particles with positive or negative effective mass, then focusing or defocusing, or in other words, attractive or repulsive, nonlinearity is required to compensate for the dispersion [2]. There exist many subtle examples, where the above rule is challenged. For example, gap solitons [2] involve linear excitations with both positive and negative masses. If parametric wave mixing is present, then the nonlinearity is no longer simply attractive or repulsive, but becomes phase dependent and leads to solitons with novel properties [3]. If a system is far from an equilibrium, other unexpected localization rules can come into play. In particular, the complex one-dimensional Ginzburg-Landau equation [4] has been shown to have bright solitons with the ''wrong'' sign of dispersion. Another research direction is to investigate the formation of multidimensional LSs, when dispersion or diffraction along different directions in space can have different signs. This can be arranged by periodic modulation of linear properties, like, e.g., in periodic potentials [5], or due to interplay of spatial and temporal effects [6].

While most of the recent experimental results and theories on localized structures have been dealing with optical or matter waves, there is a growing body of research on collective nonlinear dynamics of half-light half-matter exciton polaritons in semiconductor microcavities [7]. Vortices [8], patterns [9], and solitons [10,11] have been studied in the context of microcavity polaritons. In particular, our recent work [11] has predicted the existence of one-dimensional bright polariton solitons in microcavities. The mechanism of formation of these structures is similar to that of conventional (light only) cavity solitons [12,13], but bears important polariton features. In particular, it is essential for the polariton soliton existence that they have a sufficiently large momentum, so that the effective mass along the direction of motion changes from positive to negative and thus allows for the compensation of the polariton-polariton repulsion. The effective mass along the orthogonal direction remains positive, and therefore the dispersive spreading of the two-dimensional polariton wave packet in the direction orthogonal to its velocity is expected. In fact, to combat this spreading we have previously proposed to use polariton waveguides [11]. However, recent experiments [14] addressing superfluidity of microcavity polaritons reported some evidence of a remarkable concurrent phenomenon of the suppressed and probably canceled polariton dispersion along both directions in the cavity plane. Dispersion cancellation has manifested itself in the formation of a moving 2D localized polariton structure without any confining potential [14].

Our present theoretical study confirms the existence of 2D cavity polariton solitons (CPSs) and initiates the discussion of their complex physics. This is so far a unique example where the existence of self-localized states in a nonequilibrium optical or condensed matter system with opposite dispersion signs along the two orthogonal directions is supported experimentally and theoretically. The coupled dynamics of the linearly polarized (in the cavity plane) photon E and of the quantum well exciton Ψ field amplitudes is governed by the following dimensionless system of equations [7,11]

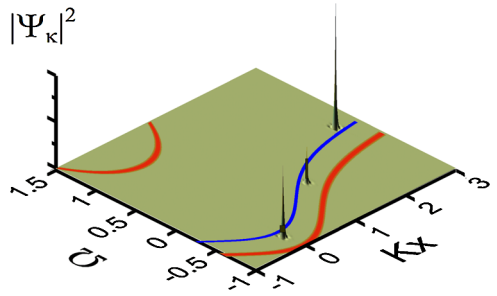

FIG. 1 (color online). Red (upper and lower) and blue (middle) lines in the (Ω, k_x) plane indicate the dispersion characteristics of the linear and nonlinear polaritons, respectively. $|\Psi_\kappa|$ is the spectrum corresponding to the 1D parametric soliton shown in Fig. 6(c).

$$\partial_t E - i(\partial_x^2 + \partial_y^2)E + (\gamma_{\rm ph} - i\Delta)E = i\Psi + E_p e^{ik_p x},$$
$$\partial_t \Psi + (\gamma_{\rm ex} - i\Delta)\Psi + i|\Psi|^2\Psi = iE, \quad (1)$$

where E_p and k_p are amplitude and momentum of the external pump beam. Δ is detuning of the pump frequency from the identical resonance frequencies of excitons and cavity. $\gamma_{\rm ph}$ and $\gamma_{\rm ex}$ are the cavity and exciton damping constants. Full details of the rescaling into physical units can be found in [10,11]. A unit of t corresponds to 0.25 ps and a unit of x to ~ 1 μm, if typical parameters of polariton experiments with a single InGaAs/GaAs quantum well are assumed.

The linear polariton eigenstates in the pump free cavity ($E_p = 0$) are sought in the form $E, \Psi \sim e^{-i(\Omega-\Delta)t+ik_x x+ik_y y}$, which gives the two well-known branches of the polariton dispersion, $\Omega(k_x, k_y)$, see, e.g., [7] and the red (upper and lower) lines in Fig. 1. The upper branch ($\Omega > 1$) is irrelevant for our present study, which focuses on the lower branch ($-1 < \Omega < 0$). Note that Eqs. (1) do not account for the saturation of the photon-exciton coupling for high densities of the latter [15]. It can be shown that this nonlinear effect is important only for the frequencies matching the upper branch; therefore, it is safe to disregard it here. The curvature of the $\Omega(k_x, k_y)$ surface determines the linear 2nd order dispersion and the effective polariton mass. The repulsive nonlinearity of excitons results in the up-shift of the polariton dispersion, but retains its shape; see the blue (middle) line in Fig. 1. Fixing $k_y = 0$ (as for the pump field), one finds that the effective mass is positive for $k_x < k_d$ and negative for $k_x > k_d$ ($k_d \sim 0.885$). We have previously demonstrated that the homogeneous solution (HS) of Eqs. (1) is bistable [see Fig. 2(a)] and there exist CPSs moving with a fixed velocity V_s and nesting on the lower branch of the HS bistability loop, provided $k_p \geq k_d$ [11]. Using the terminology of Ref. [14] we work in the regime of the triggered optical parametric oscillator, when the instability of the HS does not grow out of noise, but can be induced by a seed pulse. The CPS in Fig. 2(b) moves with the velocity 2×10^6 m/s. It traverses across the typical pump spot of 100 μm in 50 ps or 200 of adimensional time units.

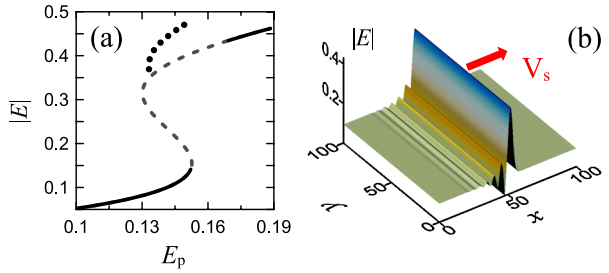

FIG. 2 (color online). (a) Bistability loop of the homogeneous solution (HS). The dashed line corresponds to the unstable HS. The dotted line marks the maximum intensity of the 1D CPSs localized along x, as shown in (b). (b) Soliton stripe moving in the x direction with velocity $V = 0.56$. Parameters: $E_p = 0.139$, $\Delta = -0.25$, $k_p = 1.2$, $\gamma_{\rm ph} = \gamma_{\rm ex} = 0.1$.

To find stable 2D CPSs we proceed by taking 1D CPS as in Ref. [11] and extend it to infinity along the y axis; see Fig. 2(b). Then we bind the soliton stripe by multiplying it with a broad but finite in y tophat function. As a result the stripe edges start moving with velocity V_f along y forming the moving fronts, Fig. 3(a). $V_f \neq 0$ does not result in the motion of the soliton center of mass (since two edges move in the opposite directions), while $V_s \neq 0$ does. The front in Fig. 3(a) is analogous to the fronts connecting the upper and lower branches of the bistable HS [12]. For the these fronts there exists the well-known Maxwell point (MP), i.e., a special value of the pump, $E_p = E_{\rm MP}$, such that the front does not move [12]. For $E_p > E_{\rm MP}$ the upper state is invading the lower one, and it is vice versa for $E_p < E_{\rm MP}$; see Fig. 3. Our fronts, however, connect the 1D soliton to the lower branch of the HS; therefore, the Maxwell point is shifted away from that for HSs, $E_{\rm MP1} \neq E_{\rm MP}$. Stable multi-

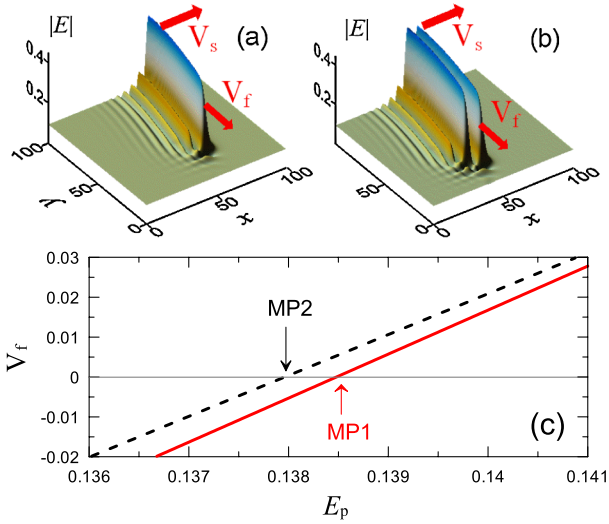

FIG. 3 (color online). Moving fronts connecting 1D single-hump (a) and double-hump (b) CPSs and HS background. (c) Velocities V_f of the single-hump (solid line) and double-hump (dashed line) fronts. $V_f = 0$ at the Maxwell points MP1 and MP2. Parameters as in Fig. 2.

hump 1D solitons also exist [16] and can be connected by a front. The Maxwell point in this case is again different; see Figs. 3(b) and 3(c).

We have also performed a similar set of simulations designed to match practical experiments. In order to achieve this we have added the term $E_0(x, y, t)e^{ik_0x-i\omega_0t}$ representing a pulse, seeding a localized excitation to the equation for E. Using an elliptically shaped Gaussian beam elongated along the y axis and having 1 ps duration, we have observed that the 1D solitons in x are easily excited and their edges (along the y direction) are either converging, so that the beam is shrinking ($E_p < E_{\mathrm{MP1}}$), or diverging ($E_p > E_{\mathrm{MP1}}$), so that the beam is expanding; see Figs. 4(a) and 4(b). Remarkably, in a narrow window of the pump amplitudes on the left from the Maxwell point the shrinking in the y direction is suppressed, so that the emerging structures remain stably localized along both spatial coordinates; see Fig. 4(c). Performing tedious numerical simulation of Eq. (1) over the time spans exceeding 10 000 adimensional units, see Fig. 4(d), we have found that the 2D CPSs with one and two humps represent stable attractors for a generic class of initial conditions within a finite interval of pump intensities; see Figs. 5(a), 6(a), and 6(b). Thus we can claim existence of the 2D CPSs under the conditions when the polariton effective masses along the orthogonal directions have the opposite signs. The seed momenta applied in our simulation were $k_0 = 0$ (seed orthogonal to the cavity plane) and $k_0 = k_p$ (seed is collinear with the pump). Both choices have led to the soliton excitation. Note, that Amo *et al.* [14] qualitatively interpreted the observed quasinondispersive propagation of the polariton wave packets in terms of straightening of the Bogolyubov dispersion [17], which is not equivalent to the soliton concept.

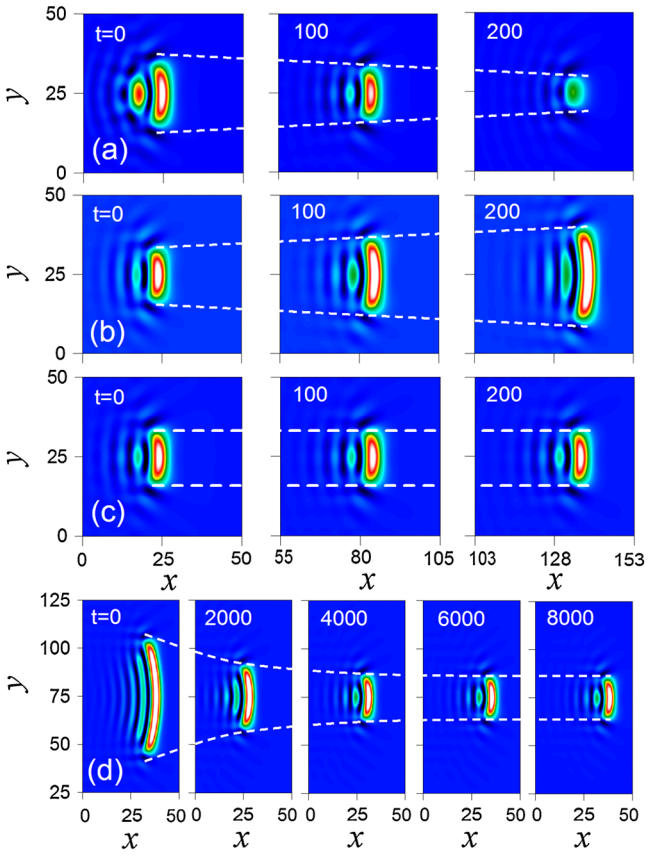

FIG. 4 (color online). (a) Shrinking of the initially localized excitation observed for $E_p = 0.136$. (b) Spreading of the initial excitation observed for $E_p = 0.141$. (c) Formation of a stable 2D CPS for $E_p = 0.1378$. (d) Long-term dynamics showing the dynamical robustness and confirming the attractor properties of 2D CPSs, $E_p = 0.1378$. Other parameters as in Fig. 2.

While the Maxwell point argument has been useful in finding 2D CPSs, it relates to a specific value of E_p and cannot explain why solitons do exist within a finite interval of E_p. Thus other physical mechanisms are likely to be involved in the soliton formation. To start uncovering them it is instructive to look at the CPS momentum space profiles; see Figs. 6(d) and 6(e). The spectrum of the single-hump CPS exhibits a maximum around the pump momentum and has two symmetric sidelobes, which are getting more pronounced in the double-hump case. This indicates that parametric four-wave mixing of polaritons [7,14,18,19] (two pump polaritons decaying into the signal and idler polaritons) plays a role in the soliton physics.

It is well known that the parametric process results in the transformation of an unstable HS into a traveling roll pattern with one of the roll sidebands picking close to the zero momentum [19]. It is well appreciated in the nonlinear optics that the nonlinearity resulting from the parametric wave mixing is not simply proportional to the polariton density but involves phases of the participating waves. The phase dependence of the nonlinearity becomes obvious after E and Ψ in Eqs. (1) are represented as superpositions of the spectrally narrow pump, signal, and idler components [19]. For example, for Ψ we have

$$\Psi = \psi_p e^{ik_px-i\delta_pt} + \psi_s e^{ik_sx-i\delta_st+i\phi} + \psi_i e^{ik_ix-i\delta_it-i\phi}. \quad (2)$$

Here $\psi_{p,s,i}$ are the slowly varying complex amplitudes and

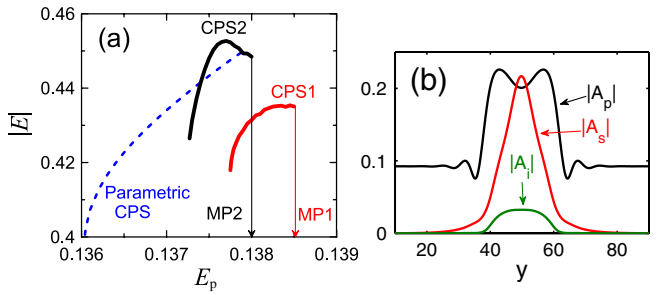

FIG. 5 (color online). (a) Maxima of $|E|$ for different soliton solutions versus the pump E_p. CPS1 and CPS2 correspond to single- and double-hump solitons as in Figs. 6(a) and 6(b), respectively. The dashed line marks a branch of the parametric CPSs; see Fig. 6(c). Parameters: $\Delta = -0.25$, $k_p = 1.2$. (b) y profiles of the pump, signal, and idler components of the photonic component of the parametric CPS from Fig. 6(c).

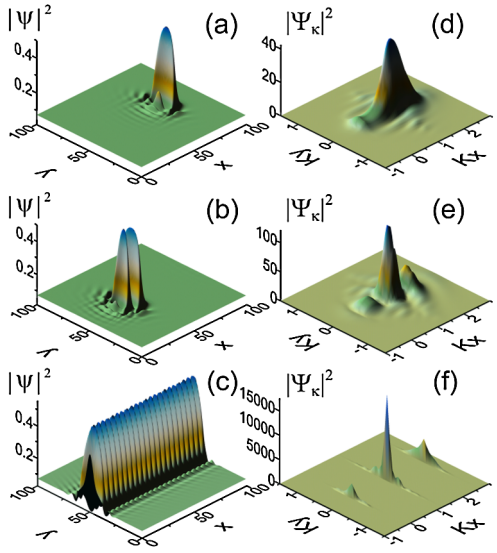

FIG. 6 (color online). Profiles of the excitonic components of the stable bright polariton solitons in the coordinate (a)–(c) and momentum (d)–(f) space. Panels (a),(b),(d),(e) correspond to the single- and double-hump 2D solitons computed for $E_p = 0.1378$. Panels (c),(f) correspond to the parametric soliton localized only along y coordinate computed for $E_p = 0.1375$. Parameters: $\Delta = -0.25$, $k_p = 1.2$.

the indices s, i correspond to the signal and idler, respectively. ϕ is the relative phase shift signifying correlation between the signal and idler fields.

Our hypothesis is that parametric nonlinearity can actually support stable localization of polaritons along the direction corresponding to the negative effective mass. The single- and double-hump CPSs are themselves not the best objects to test properties of the parametric nonlinearities, because their spectra are too broad in k_x to satisfy requirements needed for validity of the ansatz (2). In order to get narrow-band signal, idler, and pump fields, we have taken the seed pulse with $k_0 = 0$, which is infinitely extended along the x direction and localized in y. This pulse has evolved with time into a periodic in x pattern, which maintains its localization in y over the arbitrary long time intervals; see Fig. 6(c). A single-hump 2D soliton is well approximated by a single peak of this pattern. These results imply that the parametric process indeed promotes localization of polaritons along the direction corresponding to the negative effective mass. The momentum space spectrum of the periodic pattern has the expected narrow sidelobes corresponding to the signal and idler beams; see Figs. 1 and 6(f). The y dependencies of the pump (A_p), signal (A_s), and idler (A_i) components of the photonic component of the periodic pattern are shown in Fig. 5(b), where it is obvious that we are dealing here with the three component parametric 1D CPS localized along the y coordinate. Note that cavity solitons due to parametric processes have been previously discussed in the context of quadratically nonlinear materials (Ref. [20]), where an important role of the phase ϕ [see Eq. (2)] has been studied in detail.

In conclusion, we have gathered comprehensive numerical evidence unambiguously supporting the existence and practical stability of 2D solitary structures in the polaritonic microcavities; see Figs. 6(a) and 6(b). These solitons are sustained due to the interplay of the two distinct nonlinear mechanisms responsible for localization along the orthogonal directions. Localization along the direction collinear with the pump momentum happens because the dispersion induced by the negative polariton mass is balanced by the repulsive polariton-polariton interaction. Localization along the orthogonal direction, where the effective mass is positive, occurs due to parametric nonlinearity. Each of these processes taken separately supports two distinct families of 1D solitons, cf. Figs. 2(b) and 6(c). Apart from the fundamental significance of our findings, they hold a promise of practical applications. This arises from the fast and strong nonlinear response of polaritons [7], beating in these aspects the semiconductor microcavities in the weak coupling regime, where very attractive applications of 2D solitons [13] have suffered from the slow excitation times and high power demands.

[1] A. Scott, *Nonlinear Science* (Oxford University Press, Oxford, 1999).
[2] Y. Kivshar and G. Agrawal, *Optical Solitons: From Fibers to Photonic Crystals* (Academic, New York, 2001).
[3] A. V. Buryak, P. Di Trapani, D. V. Skryabin, and S. Trillo, Phys. Rep. **370**, 63 (2002).
[4] J. M. SotoCrespo, N. N. Akhmediev, V. V. Afanasjev, and S. Wabnitz, Phys. Rev. E **55**, 4783 (1997).
[5] B. Eiermann *et al.*, Phys. Rev. Lett. **92**, 230401 (2004).
[6] I. N. Towers, B. A. Malomed, and F. W. Wise, Phys. Rev. Lett. **90**, 123902 (2003).
[7] A. Kavokin, J. Baumberg, G. Malpuech, and F. Laussy, *Microcavities* (Oxford University Press, Oxford, 2007).
[8] K. G. Lagoudakis *et al.*, Nature Phys. **4**, 706 (2008).
[9] D. N. Krizhanovskii *et al.*, Phys. Rev. B **77**, 115336 (2008).
[10] A. V. Yulin, O. A. Egorov, F. Lederer, and D. V. Skryabin, Phys. Rev. A **78**, 061801 (2008).
[11] O. A. Egorov, D. V. Skryabin, A. V. Yulin, and F. Lederer, Phys. Rev. Lett. **102**, 153904 (2009).
[12] N. Rosanov, *Spatial Hysteresis and Optical Patterns* (Springer, New York, 2002).
[13] T. Ackemann, W. J. Firth, and G. L. Oppo, Adv. At. Mol. Opt. Phys. **57**, 323 (2009).
[14] A. Amo *et al.*, Nature (London) **457**, 291 (2009).
[15] R. Houdre *et al.*, Phys. Rev. B **52**, 7810 (1995).
[16] D. V. Skryabin, O. A. Egorov, A. V. Gorbach, and F. Lederer, Superlattices Microstruct. **47**, 5 (2010).
[17] C. Ciuti and I. Carusotto, Phys. Status Solidi B **242**, 2224 (2005).
[18] P. G. Savvidis *et al.*, Phys. Rev. Lett. **84**, 1547 (2000).
[19] D. M. Whittaker, Phys. Rev. B **63**, 193305 (2001).
[20] D. V. Skryabin, W. J. Firth, and A. R. Champneys, Phys. Rev. Lett. **84**, 463 (2000).